17th World Conference on Earthquake Engineering, 17WCEE
Sendai, Japan - September 13th to 18th 2020

BEHAVIOUR OF THE CENTRALISED ROCKING CONCENTRICALLY BRACED FRAME UNDER STATIC AND DYNAMIC LOADING

G. S. Djojo[(1)], G. C. Clifton[(2)], R.S. Henry[(3)], G.A. MacRae[(4)]

[(1)] *Structural Engineer, BGT Structures, Auckland, New Zealand.*
Graduated PhD Student, Department of Civil and Environmental Engineering, University of Auckland, Auckland, New Zealand, gdjo001@aucklanduni.ac.nz
[(2)] *Associate Professor, Department of Civil and Environmental Engineering, University of Auckland, Auckland, New Zealand, c.clifton@auckland.ac.nz*
[(3)] *Senior Lecturer, Department of Civil and Environmental Engineering, University of Auckland, Auckland, New Zealand, rs.henry@auckland.ac.nz*
[(4)] *Associate Professor, Department of Civil and Natural Resources Engineering, University of Canterbury, Christchurch, New Zealand, gregory.macrae@canterbury.ac.nz*

Abstract

The Centralised Rocking Concentrically Braced Frame (CRCBF) system comprises a V-braced Concentrically Braced Frame (CBF) and a centralised rocking system, integrated with energy dissipation devices. This system is designed to rock at the centre of the CRCBF and therefore, the energy dissipation devices located at the column bases are designed using Ringfeder® - Friction ring springs, each of which is configured as a double acting spring system. The double acting ring springs are pretensioned on installation to be elastically stiff up to a defined force level and then start to spring for dissipating energy in compression and tension. Besides dissipating energy, the double acting ring springs also provide a self-centring mechanism to the CRCBF. When the ring spring is fully compressed in the MCE event, the ring spring is in a lock-up state and becomes a solid steel stack. The solid ring spring does not yield but the rapidly increasing earthquake forces are now distributed to the other CRCBF components which could lead to undesirable yielding of those components, especially to those elements carrying a significant compression force. To avoid this undesirable behaviour, a machined-down threaded rod and column baseplate in each double acting ring springs system are designed to yield. A yielded threaded rod can be easily replaced by a new threaded rod and a deformed column baseplate can be repaired by straightening it. This will provide immediate occupancy performance level to buildings.

In order to investigate and validate the behaviour of the CRCBF, experimental testing was conducted utilising a half part of the bottom storey CRCBF with double acting ring springs, known as the centralised rocking frame. This was scaled down to two-thirds of the original size to fit within the laboratory test resources. The test frame of the centralised rocking frame was subjected to a series of static cyclic loading under different loading patterns and loading rates. The test frame was subsequently subjected to dynamic loading. The experimental testing demonstrated that the CRCBF performed very well with stable and repeatable flag-shaped hysteresis responses. Besides investigating the overall behaviour of the CRCBF, the behaviour of the pass-through beam-brace-column connection was also examined. The test results of the Von Mises stresses developed in the SHS column were compared with the Finite Element Analysis (FEA) results derived from ABAQUS. The direction of the diagonal tension forming in the beam-brace-column panel zone was accurately predicted by the FEA. Additionally, the Von Mises stresses derived from the FEA results showed an acceptable match with the test results with percentage differences less than 25%. Thus, this experimental testing successfully validated the behaviour of the CRCBF system.

Keywords: Low damage system; Energy dissipation devices; Double acting ring springs system; Centralised rocking concentrically braced frames; Pass-through beam-brace-column connection.

1. Introduction

Conventional ductile structures rely on system ductility and inelastic action in selected components in their lateral load resisting systems to achieve the required performance of preserving life safety in severe earthquakes. Although the ductile structures are expected to withstand severe earthquakes without loss of strength and structural integrity, the damaged structures might well have large residual deformations. In order to minimise structural damage associated with large residual deformations, low damage systems are being widely introduced in building practice. Structures with these systems are expected to withstand severe earthquakes without major post-earthquake repairs using isolating mechanisms or sacrificial systems that either do not need repair or are readily replaceable. This allows the structures to be fully operational after severe earthquakes. Centralised Rocking Concentrically Braced Frame (CRCBF) system is one of the low damage systems which has been developed and tested thoroughly under static and dynamic loading.

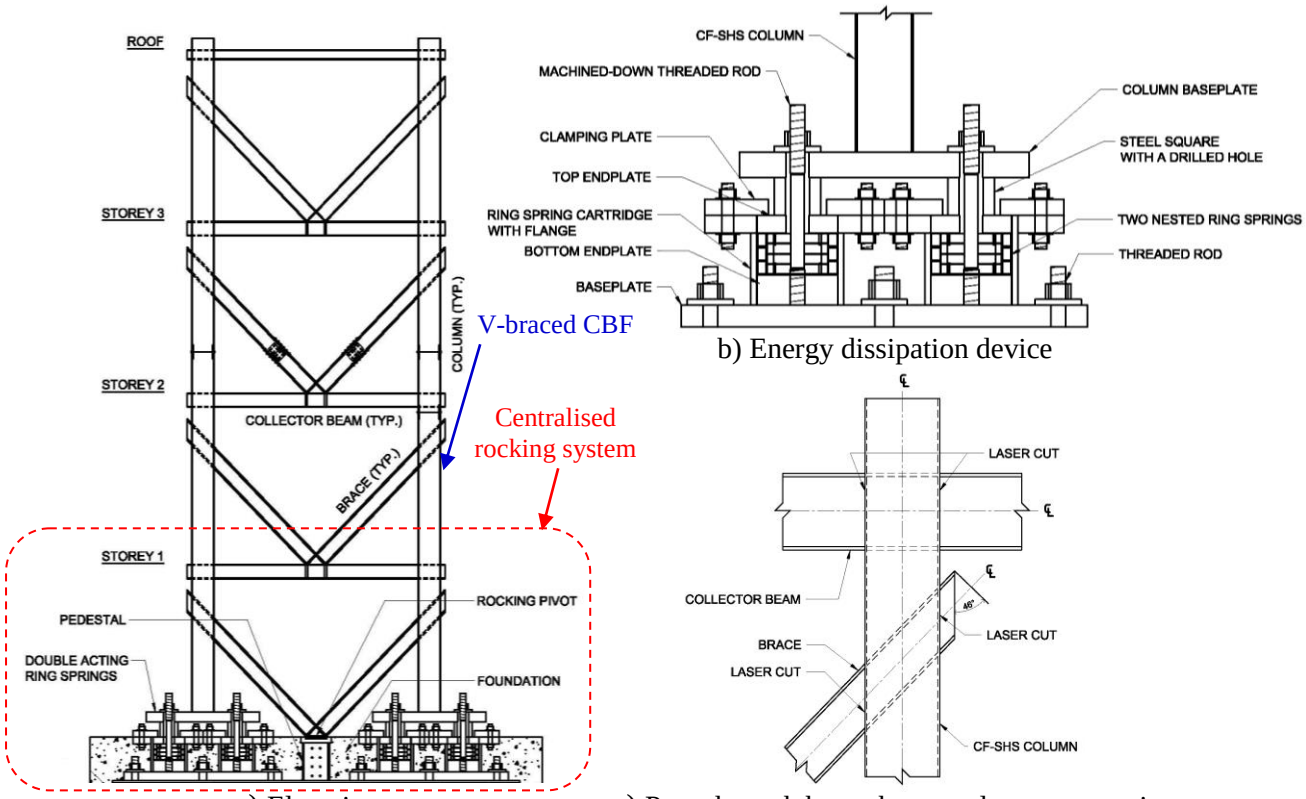

Fig. 1 – Centralised Rocking Concentrically Braced Frame (CRCBF) system

The CRCBF system (Fig.1a) comprises a V-braced Concentrically Braced Frame (CBF) and a centralised rocking system, integrated with energy dissipation devices. The system is designed and detailed to be elastically stiff under gravity loading, Ultimate Limit State (ULS) wind loading, and Serviceability Limit State (SLS) earthquake loading. It accommodates the demands under ULS earthquake loading and Maximum Considered Earthquake (MCE) loading by undergoing controlled rocking, with all components remaining effectively elastic. Then, it dependably returns to its original position following the ULS earthquakes without structural damage. Thus, the buildings utilising this system are expected to be fully operational after the ULS earthquakes and up to the MCE level. This system is designed to rock back-and-forth at the central base of the CRCBF, allowing the columns of the CRCBF to move downward and upward. Hence, under a given lateral drift, this system generates only half the magnitude of the vertical movement of the floor slab at the CRCBF edges compared to a rocking system which rotates at its corner. This will lessen displacement compatibility issues with the attached floor slabs. To accommodate the expected vertical

movement of the CRCBF columns during the ULS earthquake loading, the energy dissipation devices located at the column bases (Fig.1b) require a double acting spring system. The energy dissipation devices are also required to be very stiff under gravity loading, ULS wind loading, and SLS earthquake loading. Ringfeder ® - Friction ring springs have been chosen to be the energy dissipation device for this centralised rocking system because they can be configured as a double acting spring system to dissipate earthquake energy in both directions and can be prestressed up to a defined significant force level to provide a high initial stiffness. The ring spring also provides a self-centring mechanism to the CRCBF system.

The CRCBF is specifically designed using a square hollow section (SHS) filled with concrete for its columns, referred to as CF-SHS columns. This column design provides high column capacities in axial and bending. Additionally, the concrete core prevents premature local buckling of the SHS and acts as a heat sink to provide sufficient fire resistance [1]. For the collector beams and braces, wide-flange sections are used. Then, in order to provide a rigid connection in the beam-brace-column joint for maintaining lateral stiffness of the CRCBF, a pass-through beam-brace-column connection (Fig.1c) is introduced. The rigidity of the connections is achieved by transferring the bending moments from the collector beam or the brace to the CF-SHS column as a vertical force couple into the CF-SHS column. The shear force and the additional bending moment due to a nodal eccentricity acting in the beam-brace-column panel zone are resolved into a diagonal tension strut in the SHS and a compression strut in the concrete core. The pass-through beam-brace-column connection has been experimentally tested and thoroughly investigated using Finite Element Model (FEM) in ABAQUS.

2. System design

The CRCBF system (Fig.1a) utilises a V-braced Concentrically Braced Frame (CBF) combined with a centralised rocking system. CBF systems are chosen for the superstructure of the centralised rocking system because of their high strength and stiffness to resist lateral forces, allowing the entire frame to rock as a rigid body. Alternatively, concrete shear walls for concrete structures or timber walls for timber structures are suitable to be the lateral load resisting systems as long as the connections between the walls and the centralised rocking frame are designed and detailed appropriately. The centralised rocking system comprises a single-storey V-braced frame with a central rocking pivot and energy dissipation devices. The rocking pivot is used to transfer gravity loads and in-plane seismic base shear to the foundation and to maintain the in-plane stability of the CRCBF while allowing a small out-of-plane rotation. When subjected to ULS earthquake loading, the rocking pivot rotates about the centre of the CRCBF, generating compression and tension forces in the CRCBF columns. Therefore, energy dissipation devices located at the base of the columns are required to control the rocking by dissipating energy in compression and tension and also to provide self-centring of the CRCBF system.

Under gravity loading, the CRCBF collector beams are designed to carry all gravity loads to the CRCBF columns. The gravity loads are then transferred into the foundation through both the V brace and rocking pivot. Under lateral loading, the CRCBF system has to meet target performance levels (Fig.2), as follows:

1. Serviceability Limit State (SLS) Earthquakes and Ultimate Limit State (ULS) Winds

   The CRCBF system is stiff under SLS earthquake loading and ULS wind loading. The SLS earthquakes to NZS1170.5 [2] have an 86.5% probability of exceedance in 50% years for a normal importance structure (IL = 2).

2. Ultimate Limit State (ULS) Earthquakes

   When the intensity of the earthquake loading is greater than the SLS earthquake, the structure undergoes controlled rocking and the energy dissipation devices dissipate energy and limit the seismic actions in the superstructure in order to keep the CRCBF elastic. The energy dissipation devices also provide self-centring following the ULS earthquake. The ULS earthquakes to NZS1170.5 have a 10% probability of exceedance in 50 years for a normal importance structure.

3. Maximum Considered Earthquake (MCE) Events

When the earthquake loading exceeds the ULS earthquake, designated structural fuses are expected to yield. The other components remain elastic to avoid collapse or extensive repairs of the structures. The MCE event to NZS1170.5 has a 2% probability of exceedance in 50 years for a normal importance structure.

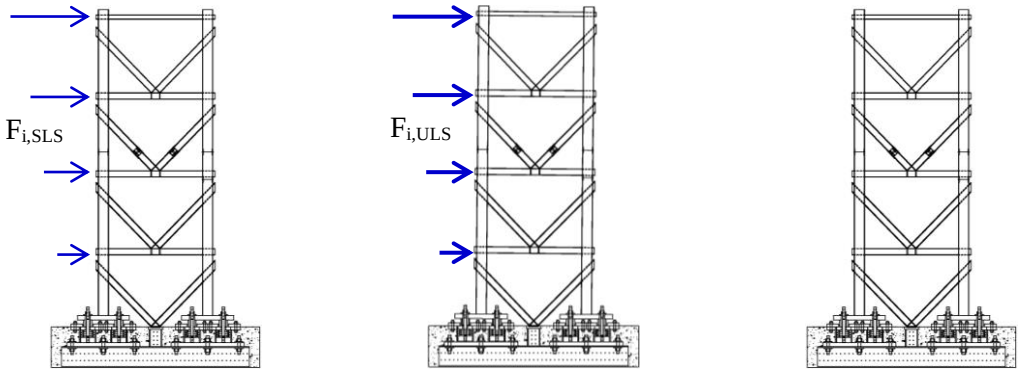

a) SLS earthquake b) ULS earthquake c) Self-centring

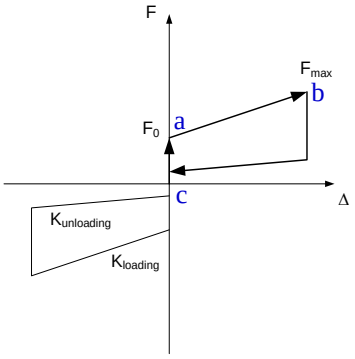

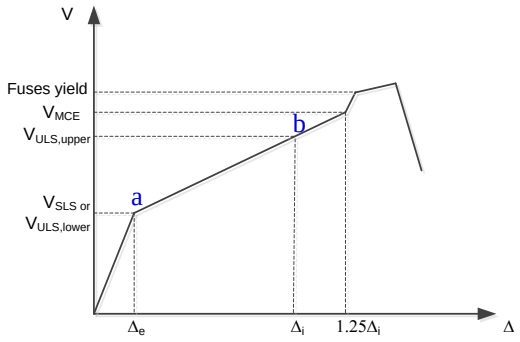

d) Flag-shaped hysteresis response e) Performance targets

Fig. 2 – CRCBF's target performance levels

3. Energy dissipation devices

3.1 Ringfeder® - Friction ring spring characteristics

The main component of the energy dissipation devices is Ringfeder ® - Friction ring spring (Fig.3a). This ring spring is a compression only spring comprising inner and outer rings that contact each other through steeply inclined contact surfaces. When the ring spring is axially compressed, the inner rings are elastically contracted circumferentially and hence develop a uniform compression stress, whilst the outer rings are elastically expanded circumferentially and hence develop a uniform tension stress [3]. Approximately, two-thirds of the input energy is dissipated by hysteretic damping during a cycle of loading and unloading. Then, one-third of the total input energy is stored elastically and released during unloading. When the ring spring is fully compressed to its rated compression capacity, F_{max}, the ring spring is locked up and behaves as a solid steel stack. The ring spring has a stable and repeatable triangular hysteresis response, as illustrated in Fig.3b.

Although the ring spring is a compression only spring, the ring spring can be configured as a double acting spring system as long as the ring spring itself is always loaded in compression. In addition to that, the ring spring can be prestressed up to a defined force level to provide a high initial stiffness. The ring springs can be arranged in parallel arrangement to increase the compression capacity of the ring springs and in series arrangement to increase the spring travel limit, as shown in Fig.3c and Fig.3d respectively. The spring

stiffness (K_{rs}), the resultant stiffness of a parallel arrangement ($K_{eff,rs,parallel}$) and a series arrangement ($K_{eff,rs,series}$) are defined in Eq. (1), Eq. (2), and Eq. (3) respectively.

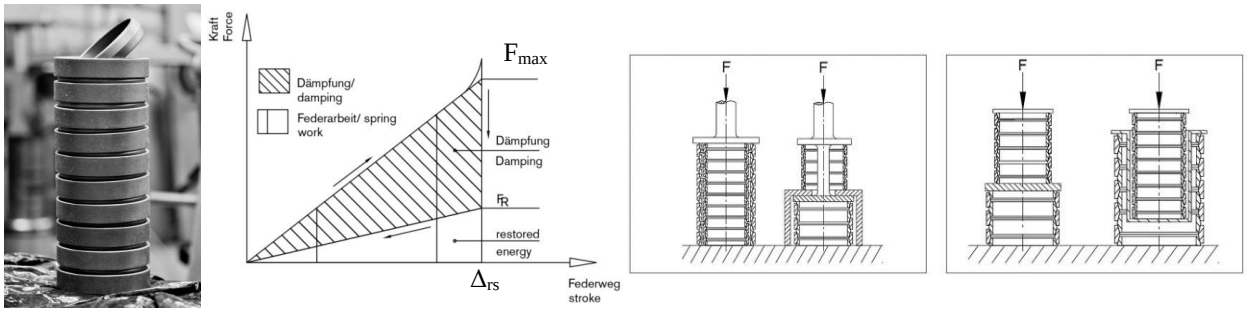

a) Ring spring b) Hysteresis response c) Parallel arrangement d) Series arrangement

Fig. 3 – Ringfeder® - Friction ring spring [4]

$$K_{rs} = F \Big/ \Delta_{rs} \tag{1}$$

$$K_{eff,rs,parallel} = K_{1,rs} + K_{2,rs} \tag{2}$$

$$\frac{1}{K_{eff,rs,series}} = \frac{1}{K_{1,rs}} + \frac{1}{K_{2,rs}} \tag{3}$$

where: F is the compression force applied to the ring spring, $K_{1,rs}$ is the spring stiffness of the first ring spring, $K_{2,rs}$ is the spring stiffness of the second ring spring.

3.2 Double acting ring springs

The double acting ring springs (Fig.1b) comprise two ring spring stacks, two machined-down high tensile threaded rods, top and bottom endplates for each ring spring, two square hollow section (SHS) cartridges for ring springs, a ring spring cartridge flange, two clamping plates, a column baseplate with two hollow section supports, and a baseplate. The two SHS cartridges arranged in parallel are welded to the baseplate and to the ring spring cartridge flange. Each ring spring stack with top and bottom endplates is put into the ring spring cartridge. The machined-down threaded rod is centrally passed through the column baseplate, the top endplate, and the ring spring. Then, it is threaded into the bottom endplate to form a connection between the bottom endplate and the column baseplate. The ring spring cartridges are then closed by the clamping plates which are bolted to the flange of the ring spring cartridge. The hollow section supports, which are part of the column baseplate, transfer the compression force to the top endplates but they can uplift. A sufficient gap has to be provided between the hollow section supports and the clamping plates to ensure the ring springs are able to displace to the maximum spring travel.

In order to meet the SLS earthquakes and ULS winds performance level, the ring springs are prestressed to 50% of the ring spring maximum compression force capacity. As the relationship between the force and the displacement of the ring springs is linear, the clear height of the cartridge can be used to define the prestressing force by measuring the spring pre-compression displacement corresponding to 50% of the total spring travel. Then, the height of the pre-compressed ring spring is used for the design height of the ring spring cartridge.

When the column is axially loaded, the column baseplate is elastically stiff up to the level of initial prestress force, and then displaces upward and downward according to the directions of the applied axial force. When subjected to a compression force, the column transfers the force to the column baseplate, allowing the column baseplate to descend. While the column baseplate is descending, the force is distributed to each hollow section support, compressing the top endplate, the ring spring, and the bottom endplate to transfer the force to the baseplate and foundation. When subjected to a tension force, the column transfers the force to the column baseplate, allowing the column baseplate to ascend, initiating gap opening, lifting up the

machined-down threaded rods and the bottom endplates, and compressing the ring springs upward. The top endplates resist the compressed ring springs and transfer the force to the ring spring cartridges through their flange. From the ring spring cartridges, the force is transferred to the baseplate and foundation. This system and similar configurations of the double acting ring spring systems have been experimentally tested under different loading rates with the range from quasi-static to seismic dynamic.

For the double acting ring springs system testing conducted at The University of Auckland, the assembled specimen (Fig.4a) consisted of two ring spring stacks with 20 rings of the Type 12400 ring spring (F_{max} = 200kN) in each stack. It was subjected to a series of static cyclic loading. This testing showed that the performance of the ring springs was independent to the loading rate with stable and repeatable flag-shaped hysteresis responses. Additionally, this system returned precisely to its initial position [5]. Fig.4b shows a good match of the hysteresis curve between the test result and the numerical prediction. This testing also confirmed the performance of the double acting ring spring systems was consistent with the past experimental testing [6, 7, 8].

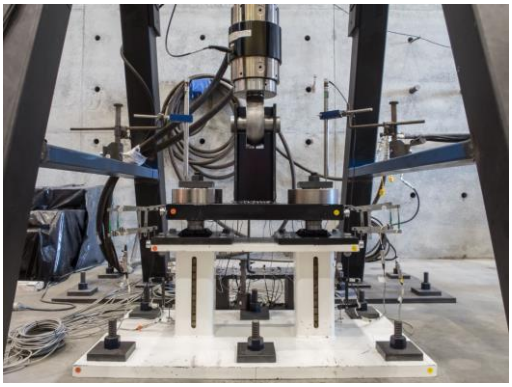

a) Assembled specimen

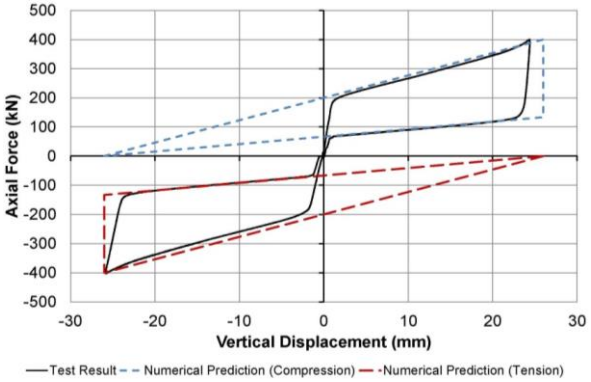

b) Hysteresis response

Fig. 4 – Double acting ring springs testing [5]

3.3 Fuse system

When the ring spring is fully compressed in the MCE event, the ring spring is in a lock-up state and becomes a solid steel stack. The solid ring spring does not yield under the increasing seismic forces and the forces are now distributed to the other CRCBF components which could lead to undesirable yielding of those components, especially to those carrying a significant compression force. To avoid undesirable behaviour of the structure due to significant tension forces, the high tensile threaded rod (Fig.5a) is designed to be a replaceable fuse by machining down it to a specified diameter. This allows yielding occurs in the shank region rather than in the threaded region. The yielded threaded rod can be unthreaded and replaced with a new threaded rod. Significant compression forces after the lock-up of the ring spring can be anticipated by designing the column base plate (Fig.5b) to deform and develop a yieldline in the column baseplate. The column baseplate is designed to be repairable by straightening the deformed column baseplate. Hence, structures with CRCBF systems are expected to be fully operational following the anticipated MCE event.

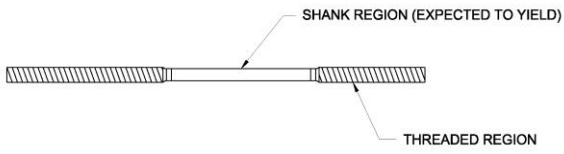

a) Machined-down threaded rod

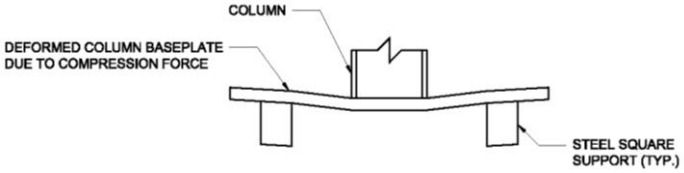

b) Column baseplate

Fig. 5 – Structural fuses

In the double acting ring springs testing, no damage or yielding was observed in the components of the double acting ring springs, except the machined-down threaded rods. The threaded rods were slightly stretched and underwent plastification in its shank region, showing the fuse system worked as intended. On

the other hand, a yieldline in the column baseplate was not shown because the column baseplate capacity was considerably greater than the applied bending moment. A supplementary finite element analysis of the column baseplate with a reduced thickness was conducted in ABAQUS to ensure the column baseplate yielded before yielding occurred in the other CRCBF components. However, this is not discussed further in this paper.

4. Pass-through beam-brace-column connection

A pass-through connection (Fig.1c) has been developed for the connection of the collector beams, braces, and CF-SHS columns in the CRCBF system to provide a rigid connection in the beam-brace-column joint for maintaining lateral stiffness of the CRCBF. The SHS column faces are cut, based on the shapes of the collector beam and brace sections. Then, the collector beam and brace are individually passed through the SHS column and are welded to the external faces of the SHS column. Lastly, the SHS column is filled with concrete to produce a robust rigid connection.

Generally, a beam-brace-column panel zone with an offset brace centreline to the beam-column joint has a high shear force and an additional bending moment to a column due to a nodal eccentricity. However, in this case, the shear force and the additional bending moment acting in the beam-brace-column panel zone are resolved into a diagonal tension strut in the SHS and a diagonal compression strut in the concrete core. As a result, the shear force and the additional bending moment due to the nodal eccentricity in the CF-SHS column are significantly reduced. The diagonal compression struts when the CRCBF is in tension and compression are illustrated in Fig.6a and Fig.6b respectively.

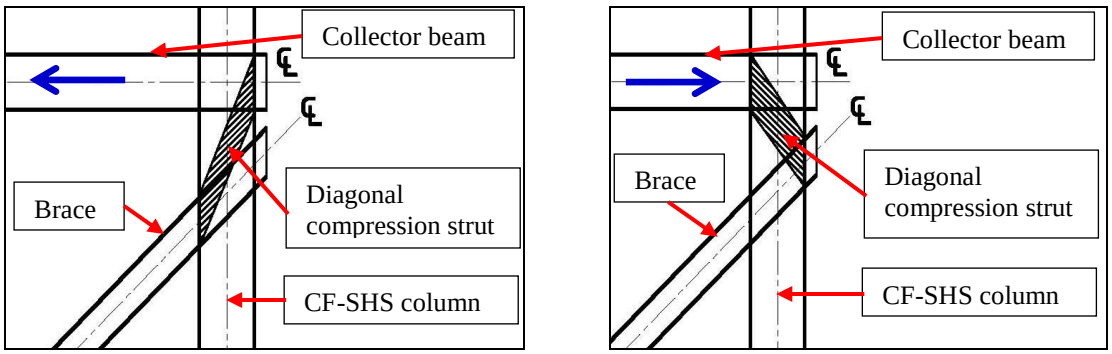

a) When the CRCBF is in tension b) When the CRCBF is in compression

Fig. 6 – Diagonal compression strut in the CRCBF column panel zone

5. Experimental validation of the centralised rocking frame

When the CBF system is incorporated with the centralised rocking system, the global behaviour of the CBF system is governed by the centralised rocking system. The CBF is expected to remain elastic during rocking with a negligible residual deformation relative to the rigid body rotation of the CBF because the ULS earthquake loading is resisted through rocking and dedicated energy dissipation devices rather than through large lateral deformations and yielding of CBF components. Therefore, this experimental testing focused on the bottom storey of the CRCBF, known as the centralised rocking frame.

The test frame of the centralised rocking frame was represented by a half part of the bottom storey CRCBF with double acting ring springs, which was scaled down to two-thirds of the original size to fit within the laboratory test resources. The assembled specimen (white frame) and the component details of the centralised rocking test frame are shown in Fig.7 and Table 1 respectively. The objectives of this testing were to observe 1) the CRCBF hysteresis loops, 2) the self-centring capability, 3) the behaviour of the centrally rocking pivot, 4) the double acting ring spring performance as the frame describes an arc during rocking, and 5) the pass-through beam-brace-column connection.

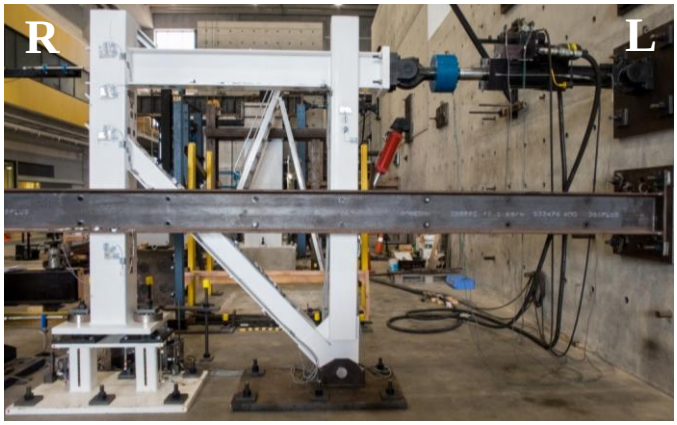

Fig. 7 – Assembled specimen of the centralised rocking test frame [9]

Table 1 – Component details for the centralised rocking test frame [9]

Components	Dimensions (mm)	Quantity
Ring spring	Type 12400	2 x (19+2 half ring)
Machined down plain class 8.8 threaded rod	Threaded region ∅30; plain region ∅24 L = 650	2
Ring spring cartridge	-	1 set
Vertical post (C450L0)	SHS 200x200x5; L = 2338	1
CF-SHS column with a column base plate and two SHS supports (C450L0)	SHS 250x250x6; L = 2209	1
Collector beam (G300)	250UB37.3; L = 2110	1
Brace (G300)	150UC30.0; L = 2522	1
Rocking pivot base plate (G300)	1200x700x50	1
AISI 4140 cylinder (Pin joint)	∅50	1
Macalloy 1030 anchor rod	∅25; L = 1000	12

note: L is the length of the component, CF is for Concrete Filled, f'_c is 50MPa

The centralised rocking test frame was subjected to a series of static cyclic loading under different loading patterns and loading rates and subsequently was subjected to dynamic loading (ie. 1940 El Centro earthquake record, 2003 Hokkaido earthquake record, and 1985 La Union earthquake record). The dynamic loading was derived from cyclic lateral displacement histories from non-linear modal time history analyses in SAP2000, scaled accordingly [9]. As the behaviour of the centralised rocking frame was always consistent and repeatable in each test, the uniform cyclic loading pattern (Fig.8a) is selected to represent the static cyclic loading and the 1940 El Centro earthquake record (PGA:0.38g) (Fig.8b) is selected to represent the dynamic loading. The structural responses due to dynamic loading are summarised in Table 2.

5.1 General test observations and results

The centralised rocking test frame performed very well under static and dynamic loading. The test results showed stable and repeatable flag-shaped hysteresis loops (Fig.9) which retained the hysteresis response of the double acting ring springs (Fig.4b). It dependably self-centred at the end of each testing, as indicated by zero residual force in the loading system at the end of the testing when the frame returned to

zero displacement. However, as the test frame rocked about the rocking pivot, the CF-SHS column described an arc relative to the rocking pivot. As a result, the axial force from the CF-SHS column was not distributed evenly between the two ring spring stacks of the double acting ring springs. Nevertheless, no stiffness or strength degradation was observed in the hysteresis responses of the centralised rocking frame.

From Fig.9, the lateral force to initiate a spring displacement in tension was 128kN. The initial stiffness and the loading stiffness were 24.7kN/mm and 4.5kN/mm respectively. When subjected to the uniform cyclic loading, the maximum lateral displacement of the frame before the lock-up of the double acting ring springs was approximately 39.4mm or 1.58% drift. The maximum applied lateral force was 300kN. When subjected to 1940 El Centro earthquake record, the test frame still generated a flag-shaped hysteresis response and the behaviour of the test frame remained the same as the test frame subjected to static loading, except the peak lateral force was 200kN. The summary of the structural responses due to dynamic loading was tabulated in Table 2.

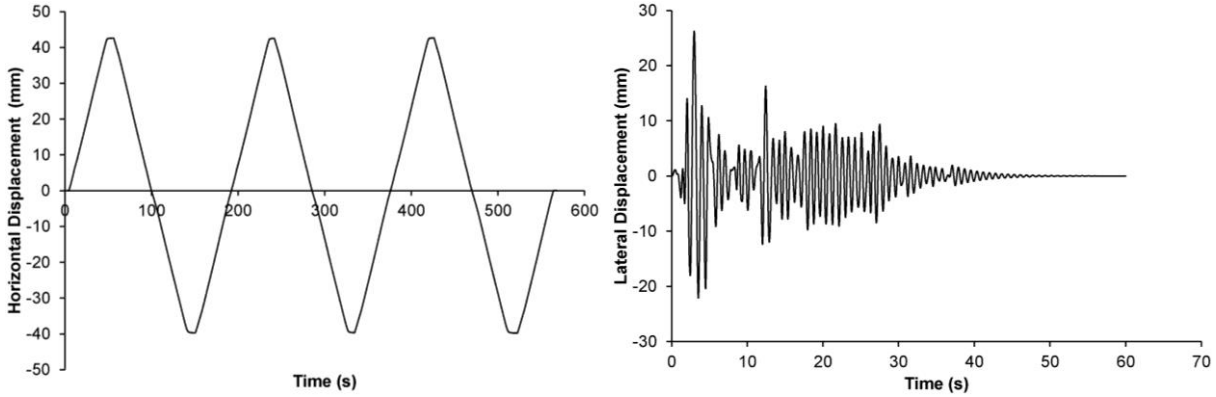

a) Uniform cyclic loading b) 1940 El Centro eq record (PGA:0.38g)

Fig. 8 – Loading protocols for static cyclic loading and dynamic loading [9]

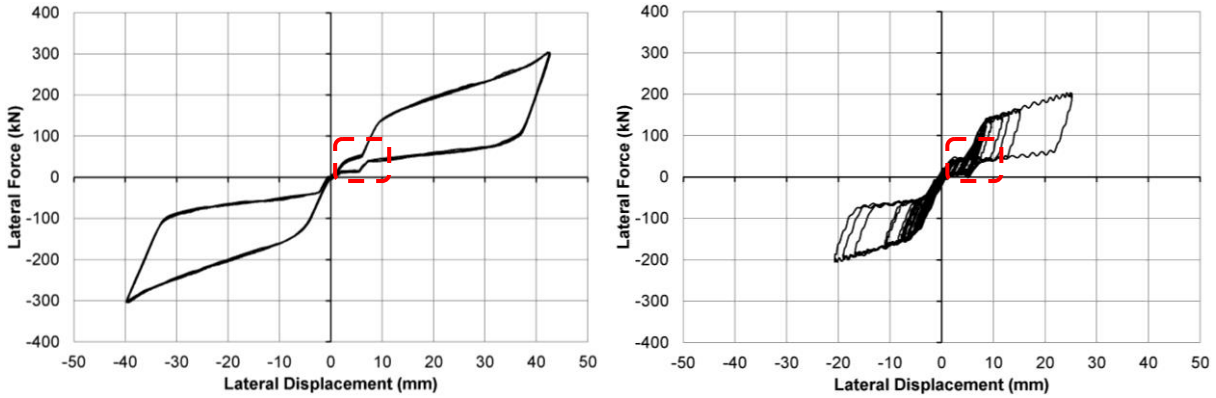

a) Uniform cyclic loading b) 1940 El Centro eq record (PGA:0.38g)

Fig. 9 – Test results of static cyclic loading and dynamic loading [9]

Table 2 – Summary of the structural responses due to dynamic loading

Record	PGA	Peak lateral force	Peak lateral displacement	Lateral drift
1940 El Centro	0.38g	200kN	39.4mm	1.58%
2003 Hokkaido	0.29g	190kN	18mm	0.72%
1985 La Union	0.27g	160kN	9mm	0.36%

No damage or yielding was observed in the steel components. The cylindrical pin joint also performed well during the rocking without any permanent deformation. However, as the guard channels were provided at the mid-height of the test frame, the paint on the CF-SHS column and the vertical post which were in contact with the guard channels was scraped a little. The guard channels also did not provide a full out-of-plane restraint. Therefore, when subjected to cyclic loading, the test frame tilted out-of-plane until the frame leaning on one side of the guard channels. This created a small bump when the frame was under compression, as shown in Fig.9.

5.2 Further investigation on the pass-through beam-brace-column connection

Strain gauge rosettes were attached on steel surfaces at three locations, collector beam-column joint zone, beam-brace-column panel zone, and brace-column joint zone. These were utilised to obtain directions and magnitudes of the principal stresses on the SHS column, as shown in Fig.10 and Table 3. Hence, diagonal tension strut in the SHS column could be observed[1]. Then, from the principal stresses, the Von Mises stresses could be determined. The strain gauge readings were obtained when the frame resisted 267kN in compression and in tension. The test results of the Von Mises stresses developed in the SHS column were then compared with the Finite Element Analysis (FEA) results derived from ABAQUS, as shown in Table 4.

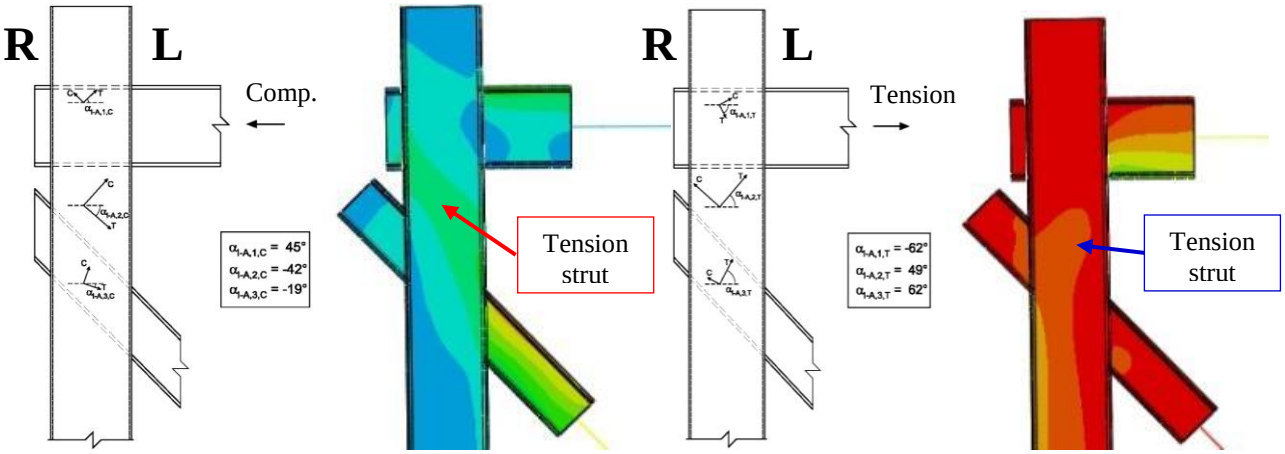

a) Test result (C) b) FEA result (C) c) Test result (T) d) FEA result (T)

Fig. 10 – Directions and magnitudes of the principal stresses in the SHS column

Table 3 – Magnitudes of principal stresses and principal angles developed in the SHS column (in MPa)

Component	Compression at 267kN			Tension at 267kN		
	ε_I (s. max)	ε_{II} (s. min)	Angle (α)	ε_I (s. max)	ε_{II} (s. min)	Angle (α)
C. beam-column joint zone	63	-40	45°	74	-42	-62°
C. beam-brace-column panel zone	196	-172	-42°	373	-196	49°
Brace-column joint zone	71	-117	-19°	266	-48	62°

Note: Column is the concrete-filled SHS column. The principal angle is the angle between the horizontal and a maximum principal stress (ε_I).

[1] As there were no instruments put in the concrete core, data for the diagonal compression strut in the concrete core were unavailable. FEA was utilised to investigate further the diagonal compression strut. The FEA results showed that the diagonal compression strut developed effectively in the concrete core by resisting a compression force greater than the SHS column.

Table 4 – Comparison of the Von Mises stresses developed in the SHS column between the test results and the FEA results (in MPa)

Component	Compression at 267kN			Tension at 267kN		
	Test result	Analysis result	%	Test result	Analysis result	%
C. beam-column joint zone	10	10	**0.0%**	14	14	**0.0%**
C. beam-brace-column panel zone	60	46	**23.3%**	86	71	**17.4%**
Brace-column joint zone	34	33	**2.9%**	50	48	**4.0%**

As shown in Fig.10, the FEA was able to accurately predict the direction of the diagonal tension forming in the beam-brace-column panel zone. When loaded in compression, the tension strut in the SHS transferred the compression force diagonally from the collector beam (R side) to the brace, generating tension in the brace. When loaded in tension, the tension strut in the SHS transferred diagonally the tension force from the collector beam (L side) to the brace, generating compression in the brace. In addition to that, the Von Mises stresses derived from the FEA results were in excellent correlation with the test results where the percentage differences do not exceed 5%, except for the Von Mises stresses in the beam-brace-column panel zone. The percentage differences in the beam-brace-column panel zone were 23.3% in compression and 17.4% in tension. The discrepancies were still considered to be acceptable as they did not exceed 25% [10]. Although some discrepancies of the Von Mises stresses between the FEA results and the test results existed, in general, the FEM of the test frame was able to demonstrate the behaviour of the pass-through beam-brace-column connection with reasonable accuracy.

6. Conclusions

The CRCBF system utilises a V-braced Concentrically Braced Frame (CBF) combined with a centralised rocking system. The centralised rocking system comprises a single storey V-braced frame with a central rocking pivot and double acting ring springs. The CRCBF system has been developed to respond the performance target of the low damage system which means the system is elastically stiff under gravity loading, ULS wind loading, and SLS earthquake loading. Then, it undergoes controlled rocking under ULS earthquake loading and MCE loading. After the ULS earthquakes, it dependably returns to its original position without structural damage and residual deformations. Thus, structures utilising this system are expected to be fully operational for an earthquake of ULS intensity or up to the MCE level.

The behaviour of the CRCBF has been comprehensively investigated through experimental testing. As the global behaviour of the CRCBF system is governed by the centralised rocking system, in the experimental testing, the CRCBF was represented by a half part of the centralised rocking frame, which was scaled down to two-thirds of the original size. The centralised rocking frame was subjected to a series of static cyclic loading under different loading patterns and loading rates and then was subjected to dynamic loading. During the testing, the CRCBF hysteresis loops, the self-centring capability, the behaviour of the centrally rocking pivot, the double acting ring springs performance, and the beam-brace-column connection were observed. The centralised rocking frame performed very well under static and dynamic loading. The test results showed stable and repeatable flag-shaped hysteresis loops which retained the hysteresis response of the double acting ring springs. The lateral force to initiate a spring displacement in tension was 128kN. The initial stiffness and the loading stiffness were 24.7kN/mm and 4.5kN/mm respectively. It also dependably self-centred at the end of each testing. No damage or yielding was observed in the steel components. The cylindrical pin joint also performed well during the rocking without any permanent deformation. Besides investigating the overall behaviour of the CRCBF, the behaviour of the pass-through

beam-brace-column connection was also examined. The principal stresses to determine Von Mises stresses were obtained from strain gauge rosettes attached on steel surfaces at three locations. The test results of the Von Mises stresses developed in the SHS column were then compared with the FEA results derived from ABAQUS. The direction of the diagonal tension forming in the beam-brace-column panel zone was accurately predicted by the FEA results. Additionally, the Von Mises stresses derived from the FEA results showed an acceptable match with the test results with percentage differences less than 25%. Thus, this experimental testing successfully validated the behaviour of the CRCBF system.

7. Acknowledgements

The first author would like to acknowledge the financial support provided during the PhD research by UoA Doctoral Scholarship, QuakeCoRE extension scholarship, and New Zealand Earthquake Commission. The support and guidance from the second, third, and fourth authors, Felix Scheibmair as the test hall manager, and Ringfeder Power Transmission GMBH are greatly appreciated. Additionally, the assistance of Ross Reichardt, Shane Smith, Jay Naidoo, Mark Byrami, and Andrew Virtue in preparing and conducting the testing is truly appreciated.

8. References

[1] Hicks SJ, Newman GM, Edwards M, Ortona, A (2002): *Corus Tubes: Design Guide for SHS Concrete Filled Columns.* The United Kingdom: The Steel Construction Institute.

[2] NZS 1170.5 (2004): *Structural Design Actions, Part 5: Earthquake Actions*. New Zealand: New Zealand Standards.

[3] Gross S (1966): *Calculation and Design of Metal Springs*. Great Britain: Chapman & Hall Ltd.

[4] Ringfeder Power Transmission GMBH (2008): *Damping Technology*. Germany.

[5] Djojo GS, Clifton GC, Henry RS (2016): Experimental Testing of Double Acting Ring Springs Type II. *Poster of QuakeCoRE Inagural Meeting 2016*, Taupo, New Zealand.

[6] Filiatrault A, Tremblay R, Kar R (2000): Performance Evaluation of Friction Spring Seismic Damper. *Journal of Structural Engineering*, **126** (4), 491-499.

[7] Hill KE (1995): *The Utility of Ring Springs in Seismic Isolation Systems*. PhD Thesis, University of Canterbury, New Zealand.

[8] Khoo HH, Clifton GC, Butterworth J, MacRae GA, Gledhill S, Sidwell G (2012): Development of the Self-Centring Sliding Hinge Joint with Friction Ring Springs. *Journal of Constructional Steel Research*, **78**, 201-211.

[9] Djojo GS, Clifton GC, Henry RS, MacRae GA (2017): Experimental Validation of Rocking CBFs with Double Acting Ring Springs. *NZSEE Conference 2017*, Wellington, New Zealand.

[10] CSI (2003): *SAP2000 CSI Software Verification Examples*. The United States of America: Computers& Structures, Inc.

